Processing and Application of Ceramics 11 [1] (2017) 1–6
DOI: 10.2298/PAC1701001C

BY-NC-ND

Phase relations in the yttria–neodymia system at 1500 °C

Olga V. Chudinovych[1,*], Elena R. Andrievskaya[1,2], Jeanne D. Bogatyryova[3], Aleksander V. Shirokov[1]

[1]*Frantsevich Institute for Problems in Materials Science NAS of Ukraine, Kiev, Ukraine*
[2]*National Technical University of Ukraine "Kiev Polytechnic Institute", Kiev, Ukraine*
[3]*Physics and Technology Institute for Metals and Alloys, Ukraine NASU, Kiev, Ukraine*

Received 25 July 2016; Received in revised form 22 September 2016; Received in revised form 15 November 2016; Accepted 18 December 2016

Abstract

The phase equilibria in the binary system Nd_2O_3–Y_2O_3 at 1500 °C were studied in the overall concentration range by means of X-ray analysis and petrography. The samples of various compositions were derived from nitrate acid solutions (prepared by dissolving neodymia and yttria powders in hot diluted nitric acid) by evaporation, drying and heat treatment at 1100 and 1500 °C. Solid solutions based on different crystalline modifications of the components were obtained. The boundaries of solubility and concentration dependence of the lattice parameters for the phases formed in the system were defined.

Keywords: *phase equilibria, yttria, neodymia*

I. Introduction

Oxides of rare earth elements (REE) have unique structural and functional properties (fire resistance, resistance to aggressive environments, high thermomechanical properties) [1–3]. Materials based on them are widely used in electronics, optoelectronics, mechanical engineering, laser technology, chemical industry, metallurgy, medicine, etc. [4,5]. The Nd_2O_3–Y_2O_3 system is of special interest and the basis for new materials.

Phase equilibria in binary Ln_2O_3–Ln'_2O_3 systems were studied and characterized by the formation of limited solid solutions based on different polymorphs of initial components. From two to five polymorphs are known for REE oxides (Ln_2O_3): low temperature hexagonal (A, space group *P63/mmm*), monoclinic (B, space group *C2/m*), low temperature cubic (C, space group *Ia3*), high temperature hexagonal (H) and high temperature cubic (X) [6–10]. The stability of the low temperature crystalline modifications of REE oxides in the temperature range of 1000–1800 °C depends on the size of the ionic radius of Ln^{3+}. Polymorphic transitions in the oxides La…Gd may be reversible (such as C $\rightleftharpoons$ H) and irreversible (C $\longrightarrow$ A, C $\longrightarrow$ B), which are studied in details by Glushkova [11,12].

Phase relations and structure of the phase formed in the Nd_2O_3–Y_2O_3 system were studied by different authors [13–18]. Liquidus is characterized by peritectic type reaction between liquid and solid phases (L + H $\rightleftharpoons$ X) at 2370 °C for 84 mol% Y_2O_3, and the point of minimum melting temperature is at ~2250 °C for 30 mol% Y_2O_3. In the Nd_2O_3–Y_2O_3 system, the continuous series of solid solutions of H-type as well as limited solid solutions based on X-, A-, B- and C-REE oxide polymorphs are formed, which react between each other in solids by eutectoid C $\rightleftharpoons$ H + B and peritectoid H $\rightleftharpoons$ A + B types of transformations. Phase equilibria had been most thoroughly investigated at high temperatures (2000–2400 °C). Only a limited number of publications [13,14] can be found at temperatures below 1900 °C, but data for both variants of phase diagram were shown hypothetically with dashed lines and defined with low accuracy. Phase reactions in the Nd_2O_3–Y_2O_3 system at temperatures 1300–1600 °C have been studied experimentally and thermodynamic assessment was done as well [15]. The boundary of the phase field was defined for C-Y_2O_3 solid solution with 35 mol% Nd_2O_3 and at 1300–1600 °C and two-phase field (C + B) with 50 mol% Nd_2O_3 with low accuracy [15], where the concentration step was taken from 10 to 20 mol%. The homogeneity field extension for B-Nd_2O_3 was not defined experimentally, but was

*Corresponding author: tel: +380 44 4242271,
fax: +380 44 4242131, e-mail: *chudinovych_olia@ukr.net*

calculated through the Thermo-Calc [10]. These data were in a contradiction with previously published results [13,14], thus both have to be verified before developing ternary phase diagrams grounded on proper binary system knowledge. Thus, the study of phase equilibria in the binary Nd_2O_3–Y_2O_3 system is urgent and requires further research.

In the present paper, the interaction between yttria and neodymia at 1500 °C in the overall concentration range has been studied.

II. Experimental procedure

Yttrium oxide, Y_2O_3, neodymium oxide, Nd_2O_3 (all 99.99% produced by Merck Corp.) and analytical grade nitric acid were used as the starting materials. The neodymia and yttria powders were preliminary dried at 200 °C for 20 h followed by dissolving in hot diluted nitric acid (1:1). The Nd_2O_3–Y_2O_3 samples were prepared in concentration step of 1–5 mol% from nitrate solutions with their subsequent evaporation and decomposition at 800 °C for 2 h. The prepared powders were uniaxially pressed at 10 MPa into pellets of 5 mm in diameter and 4 mm in height. To study phase relationships at 1500 °C the as-prepared samples were thermally treated in two stages: at 1100 °C (for 1626 h in air) and then at 1500 °C (for 60 h in air) in the furnaces with heating elements based on Fecral (H23U5T) and Superkanthal ($MoSi_2$), respectively. The heating rate was 3.5 °C/min. The two-step annealing allows removing residuals of nitrogen oxides from the samples, but it is also positive for preliminary densification and following homogenization at 1500 °C. Annealing of the samples was continuous. Cooling was carried out within the furnace.

The phase composition of the samples was studied by X-ray diffraction (XRD, DRON-3, Burevestnik, Leningrad), petrographic (MIN-8, optical microscope), microstructural phase and electron microprobe X-ray (JUMP-9500 F, JEOL-Japan, INCA Penta FET ×3, Oxford Instruments) analyses.

The X-ray analysis of the samples was performed by powder method using DRON-3 at room temperature (CuKα radiation) with step size of 0.05–0.1 degrees in the range 2θ = 15–90°. Lattice parameters were refined by the least squares fitting using the LATTIC code. The algorithm of the Lattic code is grounded on regression analysis of diffraction data. The accuracy in the lattice parameter of cubic phases was within 0.0002 nm. Phase composition has been determined in accordance with the International powder standards (JSPDS International Center for Diffraction Data 1999).

The composition of the samples was monitored by spectral and chemical analysis selectively. The petrographic studies of annealed samples were carried in polarized light. The optical characteristics were specified in polarizing microscope MIN-8 with the aid of highly refractive immersion liquids.

Microstructures were examined on polished sections and rough fractured surfaces of annealed samples in backscattered electron (COMPO) and secondary electron (SE) modes by electron-probe X-ray microanalysis (EPXMA).

Stoichiometric composition was controlled selectively by chemical and X-ray fluorescence spectrum analysis.

III. Results and discussion

Studies on solid phase interaction of Nd_2O_3 (hexagonal modification, A) and Y_2O_3 (cubic modification, C) at temperature of 1500 °C has shown that the Nd_2O_3–Y_2O_3 system consists of three types of solid solutions, based on hexagonal modification (A-Nd_2O_3), monoclinic modification (B-Nd_2O_3), cubic modification (C-Y_2O_3), separated by the two-phase fields (A + B) and (B + C) (Fig. 1).

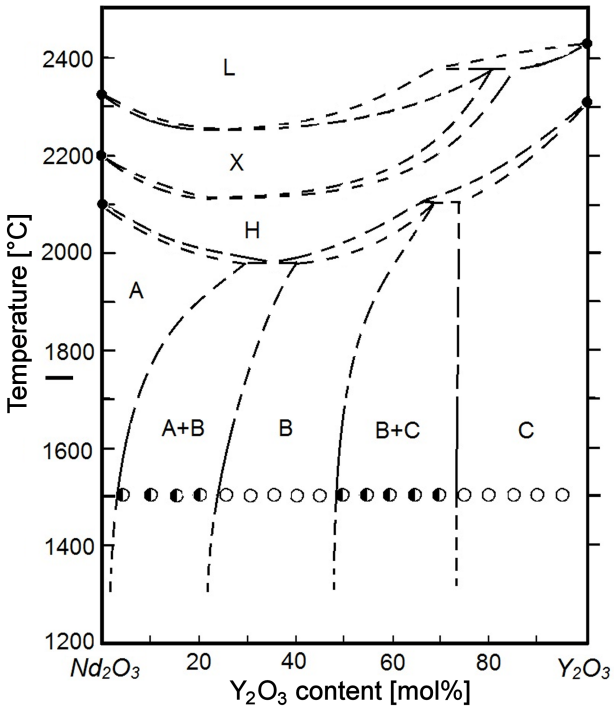

Figure 1. Phase equilibria in the Nd_2O_3–Y_2O_3 system at 1500 °C (○ - single-phase samples; ◐ - two-phase samples)

The output chemical and phase composition of the samples annealed at 1500 °C and the lattice parameters of the equilibrium phases at the given temperature are shown in Table 1. The concentration dependences of the lattice parameters of the solid solutions based on C-Y_2O_3 and B-Nd_2O_3 are shown in Fig. 2.

The boundaries of the homogeneity field of the solid solutions based on A-Nd_2O_3, B-Nd_2O_3 and C-Y_2O_3 have been determined by the boundary compositions that contain: 0–4 mol% Y_2O_3 for the phase field (A*); 5–20 mol% Y_2O_3 for the two-phase field (A* + B); 20–45 mol% Y_2O_3 for the phase field (B); 50–70 mol% Y_2O_3 for the two-phase field (C + B) and 75–100 mol% Y_2O_3 for the phase field (C). These data have shown that the solubility of Nd_2O_3 in C-Y_2O_3 is about 28 mol%

Table 1. The chemical and phase compositions, volume of the phases, lattice parameters of solid solutions, in the Nd_2O_3–Y_2O_3 system at 1500 °C, annealed for 60 h (XRD and petrography data)

Composition [mol%]		Phase composition and volume of the phases [nm^3]	Lattice parameters of the phases, a ± 0.0002 [nm]						
			<A>*		<C>	<B>			
Nd_2O_3	Y_2O_3		a	c	a	a	b	c	β
100	0	<A>*(0.1335)	0.6418	0.3743	–	–	–	–	–
99	1	<A>*(0.1341)	0.6445	0.3730	–	–	–	–	–
98	2	<A>*(0.1352)	0.6457	0.3745	–	–	–	–	–
97	3	<A>*(0.1338)	0.6445	0.3716	–	–	–	–	–
96	4	<A>*(0.1344)	0.6440	0.3743	–	–	–	–	–
95	5	<A>*↓(0.1339) + <B>(0.2052)	0.6447	0.3722	–	0.6439	0.4747	0.6735	85.4005
90	10	<A>*(0.1338) + <B>↑(0.1622)	0.6430	0.3738	–	0.6347	0.3817	0.6772	81.3774
85	15	<A>*(0.1346) + <B>↑(0.1744)	0.6428	0.3762	–	0.6885	0.4085	0.6777	81.6374
80	20	<A>*tr + <B>(0.1895)	–	–	–	0.6889	0.4101	0.6729	94.4387
75	25	<B>(0.1900)	–	–	–	0.6895	0.4100	0.6733	94.5575
70	30	<B>(0.1902)	–	–	–	0.6899	0.4107	0.6696	94.5379
65	35	<B>(0.1888)	–	–	–	0.6902	0.4117	0.6657	95.1672
60	40	<B>(0.1882)	–	–	–	0.6880	0.4124	0.6627	94.9884
55	45	<B>(0.1867)	–	–	–	0.6881	0.4135	0.6591	95.4122
50	50	<B>↓(0.1869) + <C>(1.2213)	–	–	1.0689	0.6897	0.4139	0.6578	95.6320
45	55	<B>↓(0.1861) + <C>↑(1.2357)	–	–	1.0731	0.6873	0.4131	0.6584	95.3674
40	60	<B>↓(0.1773) + <C>↑(1.2305)	–	–	1.0716	0.6660	0.4038	0.6593	89.1780
35	65	<B>tr + <C> (1.2288)	–	–	1.0711	–	–	–	–
30	70	<B>tr + <C> (1.2302)	–	–	1.0715	–	–	–	–
25	75	<C> (1.2172)	–	–	1.0677	–	–	–	–
20	80	<C> (1.2141)	–	–	1.0668	–	–	–	–
15	85	<C> (1.2039)	–	–	1.0638	–	–	–	–
10	90	<C> (1.1995)	–	–	1.0625	–	–	–	–
5	95	<C> (1.1954)	–	–	1.0613	–	–	–	–
0	100	<C> (1.1924)	–	–	1.0604	–	–	–	–

*Under given conditions (T = 1500 °C, 60 h, in air) the hexagonal A-Nd_2O_3 cannot be fixed, the hexagonal phase of A-$Nd(OH)_3$ is formed instead: <A> – solid solution based on hexagonal modification of Nd_2O_3; <C> – solid solution based on cubic modification of Y_2O_3; <B> – solid solution based on monoclinic modification of Nd_2O_3; tr – traces; ↑, ↓ – increase and decrease of the phase amount.

at 1500 °C (60 hours). The lattice parameter increases from a = 1.0604 nm for the pure Y_2O_3 to a = 1.0711 nm for the boundary solid solution.

The solubility of Y_2O_3 in the hexagonal A-Nd_2O_3 modification is ~4 mol% Y_2O_3. In accordance with the XRD phase analysis, in the samples containing from 80 to 100 mol% of Nd_2O_3 (1500 °C), instead of the hexagonal modification of A-Nd_2O_3, the hexagonal neodymium hydroxide A-$Nd(OH)_3$ was observed as soon as neodymia absorbs water from wet air and transforms into hydroxide. The lattice parameters are changed from a = 0.6418 nm, c = 0.3743 nm for the pure A-$Nd(OH)_3$ to a = 0.6447 nm, c = 0.3722 nm in the two-phase sample (A + B) containing 95 mol% Nd_2O_3.

Key difference from the literature data concerns homogeneity field size for the B-phase. In the present research, the boundary compositions have been defined

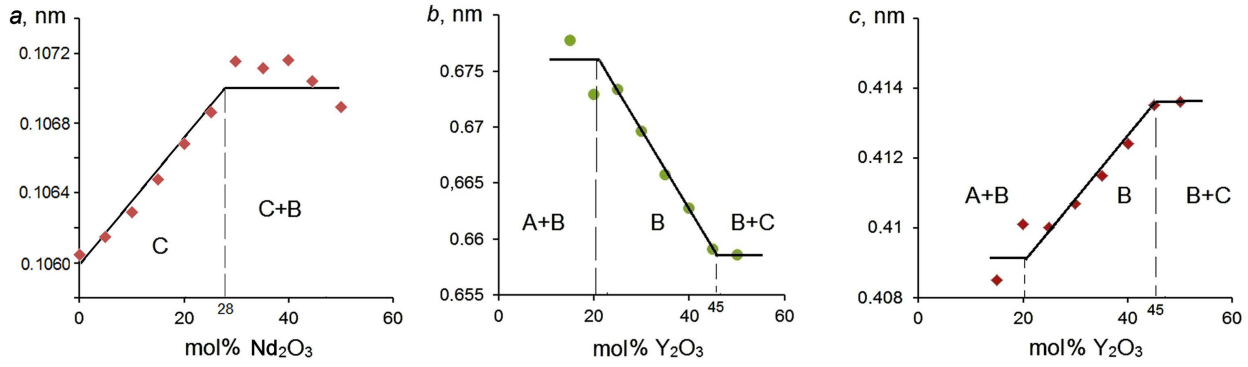

Figure 2. Concentration dependences of the lattice parameters for solid solutions based on C-Y_2O_3 (a) and B-Nd_2O_3 (b, c) in the Nd_2O_3–Y_2O_3 system heat-treated at 1500 °C

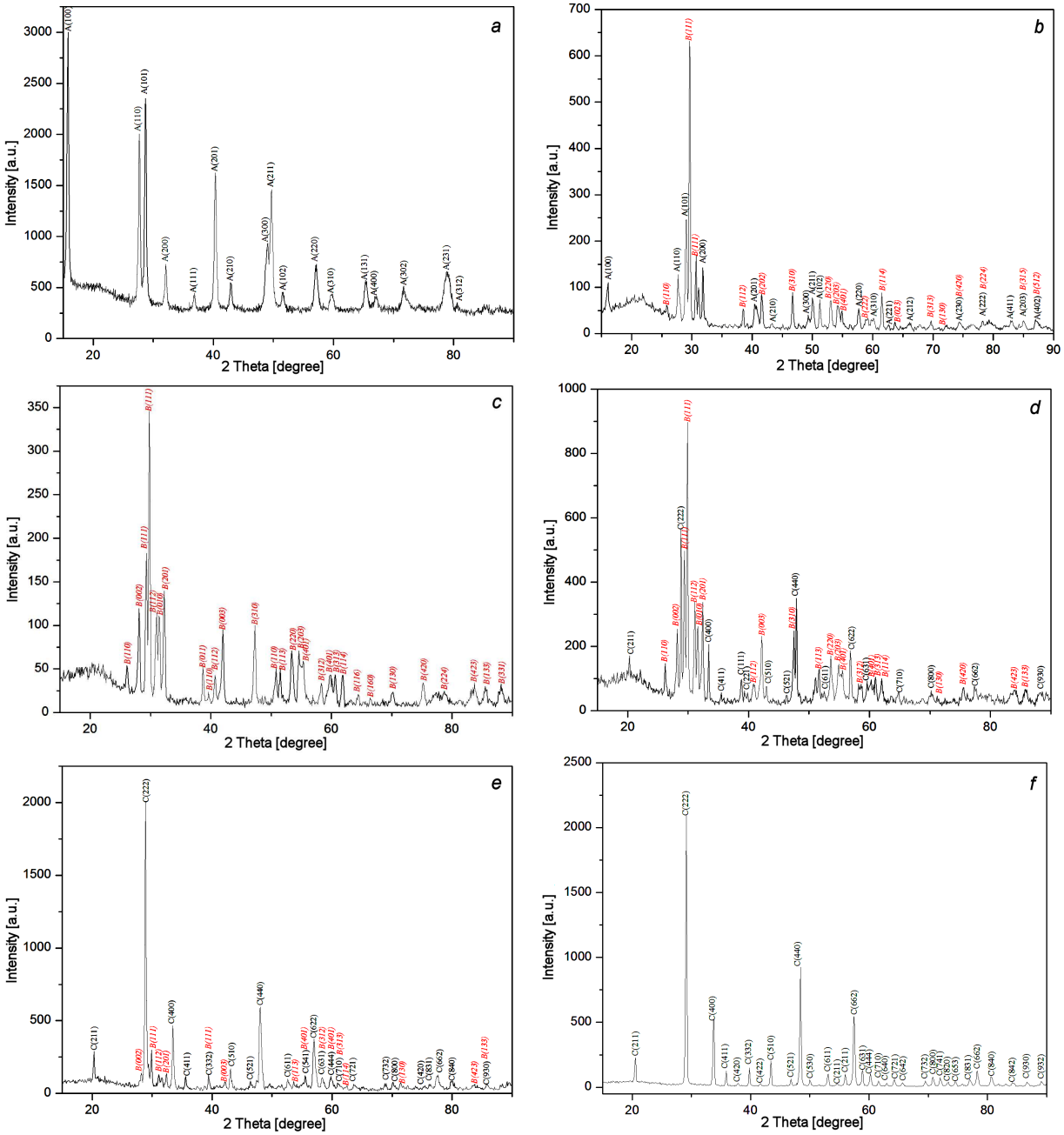

Figure 3. XRD patterns of the samples from the Nd_2O_3–Y_2O_3 system annealed at 1500 °C: a) 99 mol% Nd_2O_3 (A^*); b) 85 mol% Nd_2O_3 ($A^* + B$); c) 65 mol% Nd_2O_3 (B); d) 50 mol% Nd_2O_3 ($B + C$); e) 40 mol% Nd_2O_3 ($B + C$) and f) 15 mol% Nd_2O_3 (C)

as 20 and 45 mol% Y_2O_3 using XRD and petrography data. The low solubility limit of yttria in B-neodymia was defined after recognition of two phases in polarized light in the sample containing 20 mol% Y_2O_3. Two anisotropic phases B-Nd_2O_3 and A-Nd_2O_3 with different brightness of interference co-exist in these samples. The microstructure abruptly changed in the sample with 25 mol% Y_2O_3, i.e. one phase of B-Nd_2O_3 has been revealed in microstructure of this sample. One anisotropic phase of B-Nd_2O_3 has been found in the sample containing 45 mol% Y_2O_3, while in the 50 mol% Y_2O_3 sample, anisotropic B-Nd_2O_3 phase was mixed with isotropic C-Y_2O_3. The monoclinic crystals of B-phase giving yellow and red interference have been mixed with white isotropic crystals of C-Y_2O_3. The exact boundaries of the B-phase homogeneity field were defined from lattice parameters shown in Figs. 2b,c. The Vegard-like behaviour of lattice parameters of B-phase allowed fixing the boundaries at 20 and 45 mol% Y_2O_3. Thus, the homogeneity field is substantially narrower than measured [13,14] and calculated [15] in the literature. It is suggested that the too wide concentration step of 10 to 20 mol% in the referred papers was the reason for low accuracy.

The diffraction patterns of the samples characterizing the phase region of the solid solutions in the Nd_2O_3–Y_2O_3 system at 1500 °C are shown in Fig. 3. The X-ray diffraction and petrography data have been

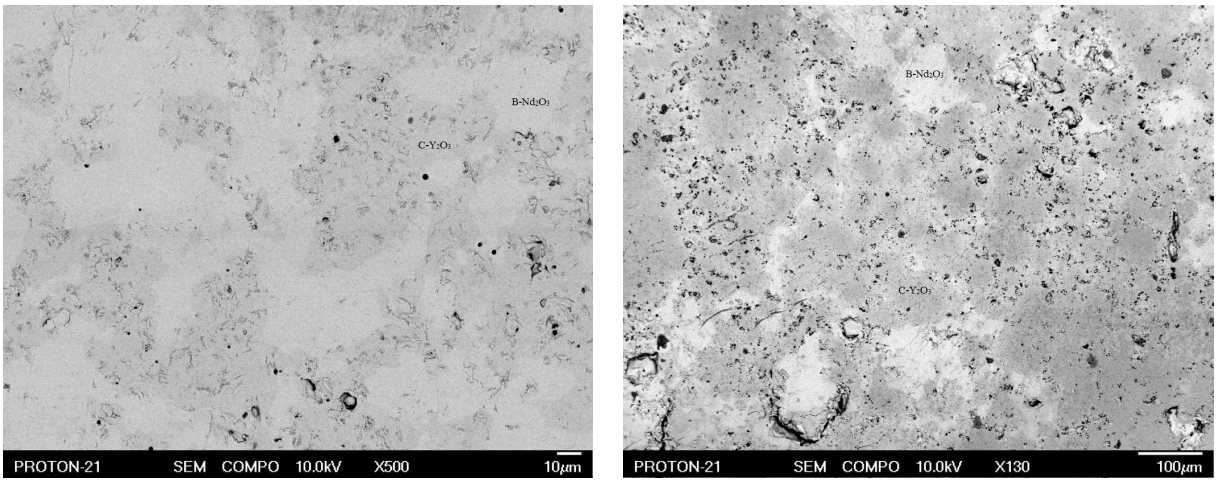

(a) (b)

Figure 4. SEM microstructures of the samples from the Nd_2O_3–Y_2O_3 system heat-treated at 1500 °C: a) 55 mol% Y_2O_3 - 45 mol% Nd_2O_3 and b) 60 mol% Y_2O_3 - 40 mol% Nd_2O_3 (light phase – <B-Nd_2O_3>, gray phase – <C-Y_2O_3>, black – pores)

completed by the electron microscopy results (Fig. 4). It was established that in the concentration range of 50 to 70 mol% Y_2O_3, the isotropic phase of C-Y_2O_3 was clearly identified in the anisotropic B-Nd_2O_3 phase. The amount of anisotropic phase B-Nd_2O_3 is significantly reduced with increasing of yttria concentration. The microstructures of the two-phase (B + C) boundary samples are shown in Fig. 4. In the samples containing 55 mol% Y_2O_3–45 mol% Nd_2O_3 and 60 mol% Y_2O_3–40 mol% Nd_2O_3, two structural components appear which differ markedly by contrast. The light phase is a matrix, and according to the local X-ray analysis, it belongs to the monoclinic (B) modification of neodymium oxide (Fig. 4a and Table 2). The second phase is darker in colour and has been identified as a cubic (C) modification of Y_2O_3 (Table 2). With the decrease of neodymium oxide concentration, the content of the isotropic C-phase increases. In the samples containing 30 to 40 mol% Nd_2O_3, the cubic modification of yttrium oxide forms the matrix phase (Fig. 4b). The EPMA results for the two phase (A + B) sample with 10 mol% Y_2O_3 helped to define equilibrium compositions for A- and B-solid solutions as 4.2 mol% Y_2O_3–95.8 mol% Nd_2O_3 for A phase and 22.4 mol% Y_2O_3–77.6 mol% Nd_2O_3 for B phase, respectively (Table 2). For the sample containing 20 mol% Nd_2O_3 only one isotropic phase C-Y_2O_3 has been found. The solubility of neodymia in yttria was found to be 28 mol% at 1500 °C using combination of petrography, XRD and EPMA data. One should note that the petrography helped to recognize the traces of anisotropic B-phase embedded into the C-matrix in the sample containing 30 mol% Nd_2O_3, otherwise undefined with the XRD below its sensitivity limit. Newly found solubility is different as compared with the experimental data of Coutures *et al.* [13] and Adylov *et al.* [14], where the boundary was defined at ~35 mol% Nd_2O_3 by XRD analysis only using quite big concentration step of 10 mol%.

IV. Conclusions

The phase equilibria in the Nd_2O_3–Y_2O_3 system were studied at 1500 °C in the whole concentration range using XRD, petrography and microscopy observations. It has been established that the solubility boundary (studied system is characterized by three types) is localized: for hexagonal (A-Nd_2O_3) at 0–4 mol% Y_2O_3, for monoclinic solid solutions (B-Nd_2O_3) between 20 and 45 mol% Y_2O_3, and for the cubic solid solutions (C-Y_2O_3) in the concentration range of 72–100 mol% Y_2O_3, which are separated by wide two phase fields (A + B) and (B + C). In accordance with Vegard's law the lattice parameter linearly increases from a = 1.0604 nm for pure Y_2O_3 to

Table 2. Phase composition in the samples from the Y_2O_3–Nd_2O_3 system, annealed at 1500 °C for 60 h in air (EPMA data were obtained from SEM images shown in Fig. 5)

Chemical composition [mol%]		EPMA composition [mol%]				Phase
Y_2O_3	Nd_2O_3	Spectrum	Y_2O_3	Nd_2O_3	Total	
55	45	S01-S03	71.3	28.7	100.0	<C-Y_2O_3>
		S04-S06	56.4	43.6	100.0	<B-Nd_2O_3>
10	90	S01-S03	22.4	77.6	100.0	<B-Nd_2O_3>
		S07-S09	4.2	95.8	100.0	<A-Nd_2O_3>

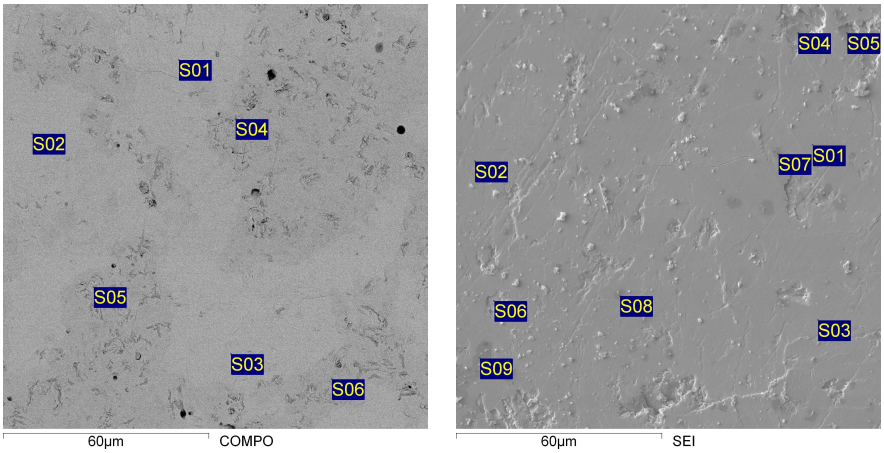

(a) (b)

Figure 5. SEM microstructures showing X-ray points used for EPMA analyses of the samples: a) 55 mol% Y_2O_3 - 45 mol% Nd_2O_3 (COMPO) and b) 10 mol% Y_2O_3 - 90 mol% Nd_2O_3 (SE)

a = 1.0711 nm for the boundary solid solution containing 72 mol% Y_2O_3.

Acknowledgements: This work was supported by Ukrainian-Indian joint R&D project, No. M/128-2016, 2015-2017.

References

1. S.F. Wang, J. Zhang, D.W. Luo, F. Gu, D.Y. Tang, Z.L. Dong, G.E. Tan, W.X. Que, T.S. Zhang, S. Li, L.B. Kong, "Transparent ceramics: Processing, materials and applications", *Prog. Solid State Chem.*, **41** (2013) 20–54.
2. J. Sanghera, S. Bayya, G. Villalobos, W. Kim, J. Frantz, B. Shaw, B. Sadowski, R. Miklos, C. Baker, M. Hunt, I. Aggarwal, F. Kung, "Transparent ceramics for high-energy laser systems", *Optical Mater.*, **33** (2011) 511–518.
3. M. Boniecki, Z. Librant, A. Wajler, W. Wesołowski, H. Weglarz, "Fracture toughness, strength and creep of transparent ceramics at high temperature", *Ceram. Int.*, **38** (2012) 4517–4524.
4. G.A. Vidrik, T.V. Soloveva, F.Ya. Haritonov, *Transparent Ceramics*, Energiya, Moscow, 1980, p. 96 [in Russian].
5. N.S. Prasad, S. Trivedi, S. Kutcher, C.-C. Wang, J.-S. Kim, U. Hommerich, V. Shukla, R. Sadangi, "Development of ceramic solid-state laser host materials", *Proc. SPIE 7193, Solid State Lasers XVIII: Technology and Devices, 71931X*, 2009 (doi:10.1117/12.813785)
6. P.A. Arsenev, L.M. Kovba, H.S. Bagdasarov, B.F. Dzhurinsky, A.V. Potemkin, B.I. Pokrovsky, F.M. Spiridonov, V.A. Antonov, V.V. Ilyukhin, *Compounds of Rare Earth Elements. Systems with Oxides of Elements of Groups I–III*, Nauka, Moscow, 1983, p. 280 [in Russian].
7. M. Yoshimura, X.-Z. Rong, "Various solid solutions in the systems Y_2O_3-R_2O_3 (R - La, Nd, and Sm) at high temperature", *J. Mater. Sci. Lett.*, **16** (1997) 1961–1963.
8. E.R. Andrievskaya, "Phase equilibria in the refractory oxide systems of zirconia, hafnia and yttria with rare-earth oxides", *J. Eur. Ceram. Soc.*, **28** [12] (2008) 2363–2388.
9. J. Coutures, A. Rouanet, R. Verges, M. Foex, "Etude a haute temperature des systems formes par le sesquioxyde de lanthane et les sesquioxydes de lanthanides. I. Diagrammes de phases (1400 °C < T < T Liquide)", *J. Solid State Chem.*, **17** [1-2] (1976) 172–182.
10. M. Zinkevich, "Thermodynamics of rare earth sesquioxides", *Prog. Mater. Sci.*, **52** (2007) 597–647.
11. V.B. Glushkova, *Polymorphism Oxides of Rare Earth Elements*, Nauka, Leningrad, 1967, p. 134 [in Russian].
12. E.R. Andrievskaya, *Phase Equilibria in the Systems of Hafnia, Zirconia and Yttria with Rare Earth Elements*, Naukova Dumka, Kiev, 2010, p. 470 [in Russian].
13. J. Coutures, R. Verges, M. Foex, "Etude a haute temperature des systemes formes par le sesquioxyde de neodyme avec les sesquioxides d' yttrium et d' ytterbium", *Mater. Res. Bull.*, **9** [12] (1974) 1603–1612.
14. G.T. Adylov, G.V. Voronov, L.M. Sigalov, "The system Nd_2O_3–Y_2O_3", *Inorg. Mater.*, **23** [11] (1987) 1146–1164.
15. S. Huang, O. Van der Biest, J. Vleugels, "Experimental investigation and thermodynamic assessment of the Nd_2O_3–Y_2O_3 system", *J. Am. Ceram. Soc.*, **89** [8] (2006) 2596–2601.
16. S.V. Chavan, S.N. Achary, A.K. Tyagy "XRD investigations in the Nd_2O_3–Y_2O_3 system and structural studies of a stabilized monoclinic phase", *J. Alloy. Comp.*, **441** (2007) 332–336.
17. S. Salehi, B. Yuksel, K. Vanmeensel, O. Van der Biest, J. Vleugels, "Nd_2O_3–Y_2O_3 double stabilized ZrO_2–TiCN nanocomposites", *Mater. Chem. Phys.*, **113** (2009) 596–601.
18. L.V. Soboleva, A.P. Chirkin, "Nd_2O_3–Al_2O_3–Y_2O_3 phase diagram and the growth of (Y,Nd)Al_5O_{12} single crystals", *Crystallogr. Rep.*, **48** [5] (2003) 945–949.
19. O. Fabrichnaya, G. Savinykh, G. Schreiber, H.J. Seifert, "Phase relations in the ZrO_2–Nd_2O_3–Y_2O_3–Al_2O_3 system: Experimental study and thermodynamic modeling", *J. Eur. Ceram. Soc.*, **32** (2012) 3171–3185.
20. S.A. Toropov, *Diagrams of the Refractory Oxide Systems*, Nauka, Leningrad, 1987, p. 822 [in Russian].